Preprint
UCRL-JC-145540

Evidence that Accelerated Proton Energy is Determined by Hot Electron Density in Targets Irradiated by Femtosecond Laser Pulses

A.J. Mackinnon, P.K. Patel, D.W. Price, S. Hatchett, M.H. Key, Y. Sentoku, C. Andersen, R. Snavely and R.R. Freeman

U.S. Department of Energy
Lawrence Livermore National Laboratory

This article was submitted to Physical Review Letters

September 24, 2001

DISCLAIMER

Evidence that accelerated proton energy is determined by hot electron density in targets irradiated by femtosecond laser pulses

A.J.Mackinnon, P.K.Patel, D.W.Price, S.Hatchett, M.H.Key

Lawrence Livermore National Laboratory, Livermore CA 94550, USA

Y. Sentoku,

Institute of Laser Engineering, Osaka University, Suita, Osaka, Japan

C.Andersen, R.Snavely, R.R.Freeman

Department of Applied Science, University of California, Davis, CA 95616,USA

ABSTRACT:

MeV proton production from solid targets irradiated by 100fs laser pulses at intensities above $1x10^{20}$ Wcm^{-2} has been studied as a function of initial target thickness. For foils 100μm thick the proton beam was characterized by an energy spectrum of temperature 1.4MeV with a cutoff at 6.5MeV. When the target thickness reduced to 3μm the temperature was 3.2± 0.3 MeV with a cut-off at 23MeV. These observations are consistent with modeling showing an enhanced density of MeV electrons at the rear surface for the thinnest targets, which predicts an increased acceleration and higher proton energies.

PACS numbers: 52.50.Jm, 52.40.Nk, 52.40.Mj, 52.70.Kz

The generation of multi-MeV proton and ion beams in high intensity interactions of ultra-short laser pulses with solid targets is a rapidly growing research area. Distinctly collimated beams with cut-off energies as high as 55MeV have been observed at high laser intensities [1-4]. The remarkable collimation, high cut-off energy and emission from the un-irradiated rear of the target distinguish these beams from the less directed, lower energy protons observed in earlier work at lower laser intensity [5,6]. Since their discovery there have been conflicting interpretations of the available experimental evidence, and two different theoretical models of the origin of these protons have emerged: One suggesting that protons are accelerated from the front [2] and the other the rear [1] of the target. Recent work has given support to the rear surface model. In particular one recent experiment has shown that the proton beam can be eradicated by introducing a small preformed plasma on the rear of the target, which is consistent with the rear surface acceleration mechanism [7,8]. In addition the annular angular pattern of proton emission, which was interpreted initially as evidence for the front surface acceleration model [2] was recently explained in a comparison of experimental data and 2D Particle In Cell (PIC) simulations [4], as due to a toroidal magnetic field formed outside the rear surface of the target. 3D PIC code simulations also shows that the highest energy protons are accelerated at the rear surface [9].

We report a different, but complementary study of the acceleration mechanism by observing the dependence of the proton energy on the thickness of the target. If the protons were accelerated, for example to 20MeV from the front of the target, then an increase in the thickness would result in a reduction of the proton energy consistent with the known energy loss of protons in the target material. For example, the stopping distance for protons of 20MeV in cold aluminum is approximately 1mm [10]; the beam would be completely stopped by a target thickness of this order. Conversely, fields that accelerate protons electrostatically from the back of the target depend strongly on the hot electron density at the rear surface [8]. As the target thickness increases then one may expect that the maximum beam energy would be reduced as the hot electrons fill a larger volume at lower density producing weaker accelerating fields.

This letter reports an investigation of the influence of target thickness on energetic proton production by ultra intense laser interaction with thin aluminum foils, which is the first to identify the important role played by electron time of flight and its effect on hot electron density driving the proton acceleration. The experimental measurements show a reduction in the peak proton energy from 23 to 6.5MeV as the target thickness is increased from 3 to 100μm. This observed reduction in beam energy with thickness cannot be explained by classical slowing of protons accelerated from the front surface, laser interaction region. However, it is consistent with acceleration from the rear surface of the target, where the time of flight of the hot electrons was responsible for reduced hot electron density and the observed reduction of proton energy.

The experiment was simulated using a 2D PIC code, with an absorbing boundary condition in the longitudinal, x (laser propagation), direction and periodic boundary conditions in the transverse direction. The simulation box was 10μm wide by 50 μm long, with a mesh size of 0.01μm and mesh numbers of N_x= 5000 and N_y = 1024. The background electron density was $40n_c$ and the rear surface layer of adsorbed hydrocarbons was modeled by assuming the material was a mixture of hydrogen in aluminum (Al:H = 1:2). The peak laser intensity was 10^{20}Wcm^{-2} with duration of 100fs (square) and a 20fs rise time. The transverse profile of the focal spot was Gaussian with a diameter of 5μm, at half maximum intensity. Simulation were made for target thickness in the range 3 to 40 micron

The experiment was performed at the Lawrence Livermore National Laboratory using, a Ti:Sapphire laser operating in Chirped Pulse Amplification mode (CPA) at a wavelength of 0.8μm and duration of 100 fs [11]. The pulse was focused by an f/2 off-axis parabola (OAP) at a P polarized angle of incidence of 22 degrees onto the target with a focal spot size of 3-5 μm, full width at half maximum (FWHM). This spot contained 30-40 % of the energy, giving a peak intensity in excess of 10^{20} W/cm^2. The laser used an ASE suppression system to attain an intensity contrast ratio of 10^{10}:1 [12]. The targets were Al foils, 3mm wide, 10mm long, with a thickness that was varied from 3 to 100μm. A fraction of the compressed CPA pulse was extracted with a pick off mirror, frequency doubled using a KDP crystal and used as a precisely timed optical

probe along a direction transverse to the interaction axis. The target was backlit by the probe and imaged with a microscope objective, operating at f/4, with a magnification of 10x, resulting in a spatial resolution of 2 - 3 μm in the target plane. The relative timing of probe and interaction pulse was known to within 1 picosecond.

Radiochromic film (RCF) radiation dosimeters and CR-39 particle detectors were used to characterize the proton beam. CR-39 is a polymer particle detector in which energetic ions cause damage as they transit through the sample. Subsequent etching is then carried out to reveal the ion tracks as etched holes. CR-39 is not sensitive to either electrons or x-rays and has been widely used as a high energy ion diagnostic[2,3,5,13]. In this experiment the CR-39 was always filtered by more than 2.5mm of RCF which stopped all slower moving high z ions so only protons were recorded. RCF consists of an organic dye sandwiched between layers of plastic with a total thickness of 265μm [1]. The dye is sensitive to the total radiation dose (x-rays, ions and electrons) and has been absolutely calibrated to give the absorbed radiation dose in krads (10^{-2}J/g). The energy deposition of the protons within the active RCF layer is mainly in the Bragg peak towards the end of the stopping range, so that successive sheets respond to protons in a fairly narrow band of increasing energy . This was quantitatively evaluated using Monte Carlo modeling of proton transport through the detector package [10] (Deposited energy was measured from many layers of RCF and the best fit truncated Maxwellian energy spectrum was calculated). As RCF also responds to electrons and x-rays, the energy deposition attributed to protons has been compared to measurements by nuclear activation and CR-39 track detectors, diagnostics that are sensitive only to ions. It was found that the signal attributed to protons on the RCF correlated well with that measured by the other diagnostics [1,13].

A film pack containing RCF and CR-39 was placed 2.5cm behind the target, and aligned so that the face of the film was perpendicular to the normal to the back of the target. Aluminum filters, 18 μm thick, were placed in front of the first layer of film giving a minimum, detectable proton energy of 4.5MeV. Interferograms of the target were made 10ps before the incidence of the interaction pulse, thus permitting the measurement of any preformed plasma (scale-lengths>10μm

and density $2x0^{19}$- $2x10^{20}cm^{-3}$). The peak proton energy was measured from the depth of penetration of the proton beam through the RCF/CR-39 film pack. Fig.1 shows how the peak proton energy pack was reduced from 23.5 to 6.5MeV as the target thickness was increased from 3 to 100μm. These results were reproducible: A 100μm foil never produced more than 6.5MeV protons while the 3μm foil always produced 16-25MeV protons. The scatter in the points is seen to increase slightly for smaller thickness. It is most probable that these fluctuations are due to small variations in the level of pre-pulse, which, if large enough, can create a pre-formed plasma at the back of the thinnest targets (<10μm) and reduce the accelerating field [7].

The peak proton energies from the 2D PIC code simulations are also shown as the dotted line in fig.1. It is clear that the simulation closely follows the trend in the data with a peak energy of 23.5MeV for 3μm targets reducing to 6.5MeV for 40μm. It is also clear from the graph that there are two distinct slopes present in the simulation results and the data. For thickness less than 20μm the peak proton energy falls in a steep quasi- linear trend with increasing target thickness, while for greater thickness the slope becomes much flatter. As discussed below, these two distinct regions can be explained by the temporal dynamics of the high-energy electrons as they propagate through the target.

The simulation results for the temperature of the quasi Maxwellian proton energy spectrum also agree well with the value deduced from the experimental data. The energy deposited within each film layer was measured from the absolutely calibrated film and the best fit truncated Maxwellian energy spectrum was found by Monte-Carlo modeling. This process also gave an estimate of total number of protons. Fig 2 (a) shows the deposited energy data from this analysis for a range of target thickness. The shots analyzed are those with the highest peak proton energy for each thickness and represent an upper bound. The lines on each data set are the results computed from Monte-Carlo modeling with the best fit Maxwellian; each has a temperature and number of protons listed in the figure caption. It can be seen from 2(a) that the proton temperature decreases from 3 to 1.4MeV and the absolute number of protons in the Maxwellian fit, decreased by an order of magnitude from $2x10^{11}$ ->$2x10^{10}$ as the thickness increased from 3 to 100μm. The

temperature and peak energy were both reduced by slightly more than 30% as the target thickness was increased from 3 to 9μm. The temperature and peak energy then markedly reduced to 1.4MeV and 8MeV respectively for targets thicker than 25 μm but thereafter remained relatively constant. The temperature distributions from the PIC simulation shown in Fig 2(b) again show the same general trend, with a large reduction in proton temperature for targets thicker than 25μm compared to 3μm. For the thinnest (3μm) targets the simulation temperature is 3.6MeV – in good agreement with the experimentally measured value of 3.2MeV.

The efficiency of conversion of laser energy into proton energy is a parameter of importance for applications. We find a maximum value (integrated over all energies), for the 3 μm thick targets of 1% (0.1% at energies >7MeV). These efficiencies can be compared with earlier work with 500J, 0.5 Ps laser pulses where of 7-13% conversion of laser to proton energy was observed in CH targets, even at energies >7MeV, with a temperature of 5 MeV [1]. This difference could have important implications for optimizing proton production at high repetition rate. It is easier to produce high average power in laser pulses of lower energy, but since the efficiency of proton production seems to falls so steeply with decreasing laser energy, it may be better to use higher energy, lower repetition rate laser pulses.

This behavior is consistent with a physical model in which the proton energy is related to the electric field at the rear surface of the target, which in turn is determined by the hot electron density n_h. The instantaneous n_h at the back surface is sensitive to the time taken for the hot electrons to reach the back surface. Once the electrons reach the back surface they are reflected by the Debye sheath towards the front of the target, where they are again reflected by the front sheath, towards the rear of the target and so on. This behavior can be seen in the PIC code output of electron phase space shown in Fig.3 for electrons for (a) 5μm and (b) 20μm targets. For targets where the double transit time of the electrons is much less than the laser pulse duration, n_h is due to a superposition of electron density from electrons entering the target at intervals of the double transit time. For the thinnest targets n_h is therefore the largest. For thickness giving a double transit time exceeding the

laser pulse duration there is no density enhancement due to reflected electrons. The turnover between the two regimes will occur at a target thickness that depends on the laser pulse length.

The sheath electric field E scales as $(n_h T_h)^{1/2}$. The proton energy should scale in general either as EL or E^2t^2, where L is a characteristic length or t a characteristic time. The dynamics of the situation are subtle as the field and its spatial extent both vary in time as shown by the PIC code. This is shown in Fig.4, which plots the evolution of the electric fields at the front and back of the target for (a) a thin (5μm), (b) a thick (20μm) target. It can be seen from (a) that the field is formed on the back surface within the first 30fs, the front field follows after 60fs and the fields spread, at a velocity of 0.17c, more than 10μm into the surrounding space by the end of the simulation. It spreads quickly because the energetic ions are moving at approximately this velocity (~0.2c) away from the target surface. In contrast the lower field at the back for the 20μm foil does not form until 100fs after the start of the simulation and the field remains only 2-3 μm from the original target surface. This corresponds to a much lower proton velocity of only 0.05c, as would be expected from the reduced peak energy of the weakly accelerated protons. Fig 5 shows the temporal evolution of the maximum proton energy for increasing target thickness. For a 3μm foil the proton energy starts to increase after 30fs and reaches a peak energy of 23MeV after 250fs. For a 30μm foil the acceleration does not begin until 150fs , well after the end of the laser pulse, and the proton energy peaks at only 7MeV after 250fs.

It is clear from comparing these detailed simulations with the experimental results that the mechanism accelerating the protons is consistent with the electrostatic field due to the laser accelerated hot electrons. Furthermore new insight into the time evolution of this mechanism has emerged from a detailed comparison of these experimental results with 2D PIC simulations. These results show that the proton beam characteristics can be modified by optimizing the target parameters; for example by utilizing longer laser pulses and very thin targets to achieve higher proton energies or modifying the shape of the target to compensate for spatial gradients in the hot electron distribution. This work also strongly suggests that the current highest proton energy of 55

MeV achieved with a petawatt laser, could be substantially increased in future with an optimized combination of intensity, pulse length, target thickness and control of pre-pulses.

In conclusion experimental data characterizing proton beam generation has been obtained as a function of initial target thickness. The observed reduction in both proton temperature and cut off energy are consistent with a rear surface acceleration mechanism in which the finite time of flight of the electrons produced a density enhancement that increased proton energies for the thinnest foils. These measurements and simulations are the first detailed study to show the importance of re-circulation of the MeV electrons on the electrostatic fields that accelerate protons to multi-MeV energies.

This work was performed under the auspices of the U.S. Department of Energy by the University of California, Lawrence Livermore National Laboratory under Contract No. W-7405-Eng-48.

References

[1] S. P. Hatchett *et al.,* Phys. Plasmas **7**, 2076 (2000), R.A.Snavely *et al.*, Phys. Rev. Lett **85**, 2945 (2000).

[2] E.L. Clark *et al.,* Phys. Rev. Lett **84**, 670 (2000).

[3] A. Maksimchuk *et al.*, Phys. Rev. Lett. **84**, 4108 (2000).

[4] Y. Murakami, Y. Kitagawa, Y. Sentoku, *et al.*, Phys. Plasmas (2001).

[5] S.J.Gitomer, Phys. Fluids **29**, 2679 (1986). A.P. Fews, *et al.*, Phys. Rev. Lett **73**, 1801 (1994), F.N. Beg *et al.,* Phys. Plasmas **4**, 447 (1997).

[6] J.E.Crow, P.L. Auer and J.E.Allen J. Plasma Physics **14**, 65 (1975). J. Denavit, Phys. Fluids **22**, 1385 (1979). Y. Kichimoto, K. Mima, T. Watanabe and K. Nishikawa, Phys. Fluids **26**, 2308 (1983).

[7] A. Mackinnon *et al.*, Phys Rev. Letts. **86**,1769 (2001).

[8]. S.C Wilks *et al.,* Phys. Plasmas **8**, 542 (2001), Y. Sentoku, et al., submitted to Phys. Plasmas (2001).

[9] A. Pukhov, Phys.Rev.Lett. **86**, 3562 (2001).

[10] J.F. Ziegler, J. App Phys. **85** 1249 (1999).

[11] J.D. Bonlie *et al.*, Appl. Phys. B **70** S155 (2000).

[12] J.Itatani *et al.*, Opt Comm. 148, 70 (1998).

[13] P.K. Patel et al submitted to Phys. Rev. Lett. (2001).

Figures:

1. Peak proton energy vs target thickness for experiment and simulation. 2D PIC code results closely follow the experimental data.
2. Experimental data and 2D PIC code simulations. (a) The experimental plot shows deposited energy in RCF sheets as a function of minimum proton energy reaching each sheet for different target thickness (3μm - filled circles; 6μm - diamonds; 9 μm - open circles; 60 μm - crosses; 100 μm - triangles,). The lines are Monte-Carlo fits assuming a temperature and total number of protons in a Maxwellian as follows (3μm, 3MeV and 1.6×10^{11}; 6μm, 3.2MeV and 9.1×10^{10}; 9μm, 2.5MeV and 7.6×10^{10}; 60μm,1.4MeV and 5.1×10^{10};100μm,1.4MeV and 3.3×10^{10}). (b) The simulations show proton energy spectra from the 2D PIC model for the indicated target thickness.
3. Electron phase space from 2D PIC for 5μm target observed at 66 fs (a) and 99 fs (b). The broken lines indicate the initial target surface.
4. Contour plot of 2D PIC electric field vs time and space for (a) 5 and (b) 20 μm thick targets.
5. 2D PIC results showing proton energy vs time for increasing target thickness.

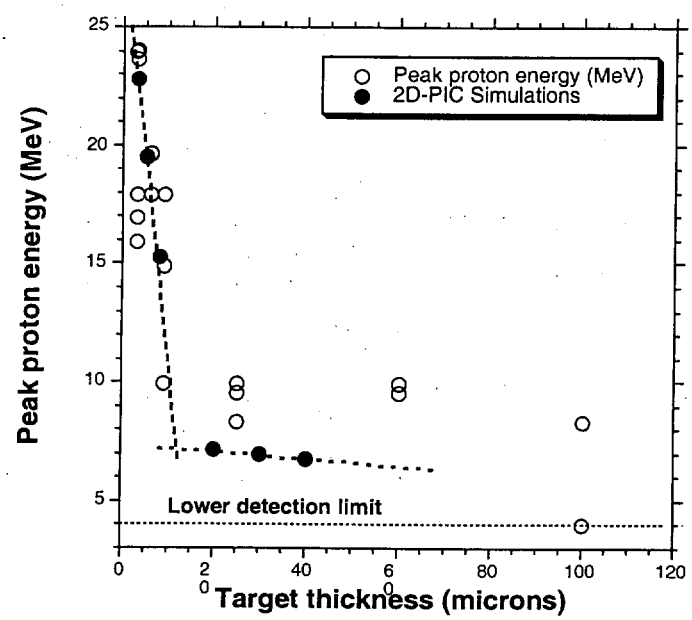

A.J.MacKinnon *et al.*, Fig. 1

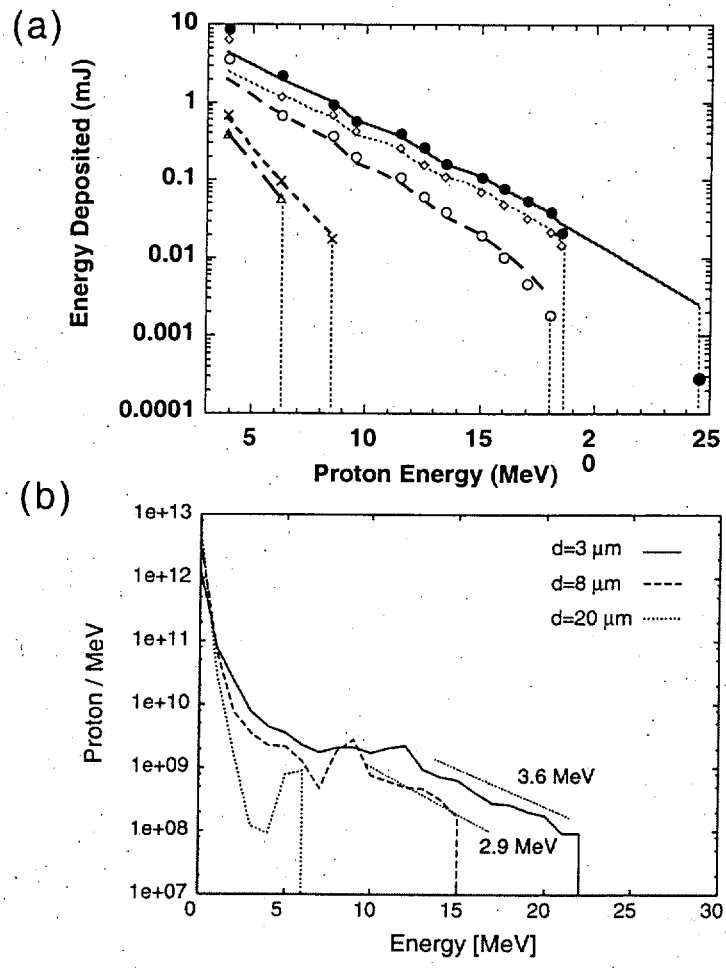

A.J.Mackinnon *et al.*, Fig. 2
(refer to figure caption for information on (a))

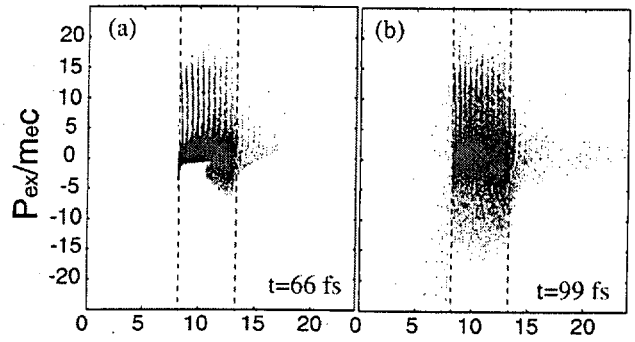

A.J.Mackinnon *et al.*, Fig. 3

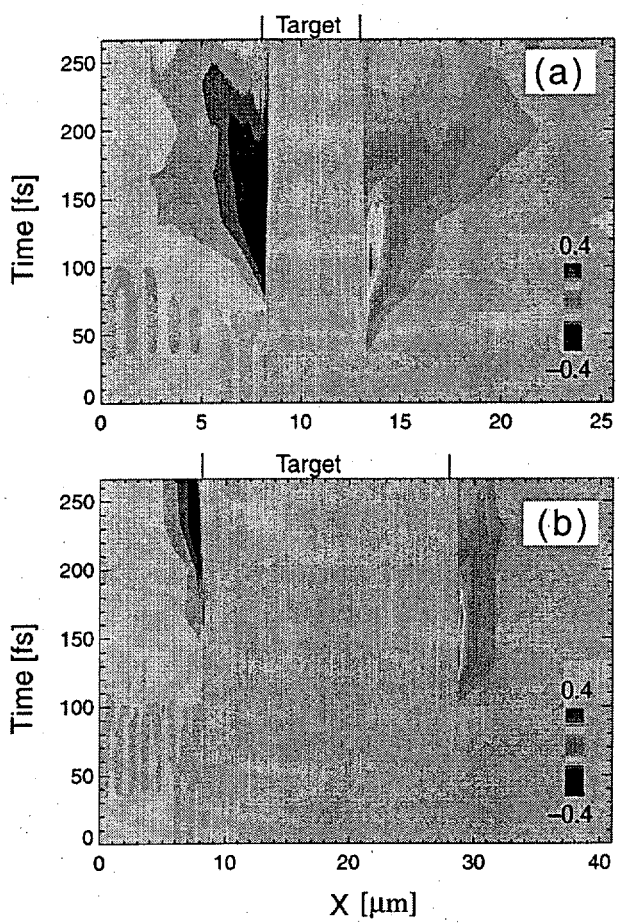

A.J.MacKinnon *et al.*, Fig. 4

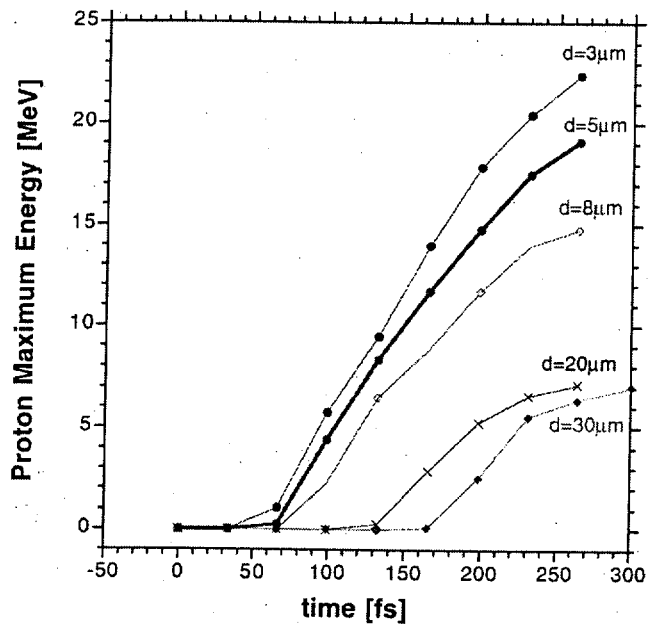

A.J.MacKinnon *et al.*, Fig. 5